PS-wave moveout inversion for tilted TI media: A physical-modeling study

Pawan Dewangan[⋆], *Ilya Tsvankin*[⋆], *Mike Batzle*[†], *Kasper van Wijk*[††], *and Matt Haney*[⋆⋆]
[⋆] *Center for Wave Phenomena, Department of Geophysics, Colorado School of Mines, Golden, CO*
[†] *Center for Rock Abuse, Department of Geophysics, Colorado School of Mines, Golden, CO*
[††] *Physical Acoustics Laboratory, Department of Geophysics, Colorado School of Mines, Golden, CO*
[⋆⋆] *Center for Wave Phenomena, Department of Geophysics, Colorado School of Mines, Golden, CO (currently at Geophysical Technology Department, Sandia National Laboratories, Albuquerque, NM)*

Summary

Mode-converted PS-waves can provide critically important information for velocity analysis in transversely isotropic (TI) media. Here we demonstrate, with physical-modeling data, that the combination of long-spread reflection traveltimes of PP- and PS-waves can be inverted for the parameters of a horizontal TI layer with a tilted symmetry axis. The 2D multicomponent reflection data are acquired over a phenolic sample manufactured to simulate the effective medium formed by a system of steeply dipping, penny-shaped cracks.

The reflection moveout of PS-waves in this model is asymmetric, and the moveout-asymmetry attributes play a crucial role in constraining the TI parameters. Applying the modified PP+PS=SS method to the PP and PS traveltimes recorded in the symmetry-axis plane, we compute the time and offset asymmetry attributes of the PS-waves along with the traveltimes of the pure SS reflections. Then the moveout attributes of the PP-, SS-, and PS-waves are inverted for the medium parameters.

Our estimates of the tilt of the symmetry axis and layer thickness almost coincide with the actual values. The inverted model is also validated by reproducing the results of transmission experiments with both P- and S-wave sources. In particular, the transmitted SV wavefield exhibits a prominent cusp (triplication) accurately predicted by the parameter-estimation results.

Introduction

Tilted transversely isotropic (TTI) models are typical for the Canadian Foothills where they cause significant mispositioning of imaged reflectors. An effective TTI medium also describes a system of parallel, dipping, penny-shaped cracks embedded in isotropic host rock (Angerer *et al.*, 2002), as well as progradational sequences.

Critically important information for velocity analysis in TTI media is provided by mode-converted PS (PSV) data. Because of the deviation of the symmetry axis from both the vertical and horizontal directions, the moveout of PS-waves from horizontal reflectors becomes asymmetric (i.e., the PS-wave traveltime does not stay the same if the source and receiver are interchanged). As demonstrated by Dewangan and Tsvankin (2004; hereafter referred to as Paper I), moveout-asymmetry attributes of PS-waves can help to constrain all parameters of a TTI layer using solely reflection data. Their algorithm, based on a modification of the so-called "PP+PS=SS" method (Grechka and Tsvankin, 2002; Grechka and Dewangan, 2003), operates with long-offset PP and PS reflections acquired in the vertical plane that contains the symmetry axis (the *symmetry-axis* plane).

Here, we process 2D multicomponent reflection data acquired over a phenolic sample and follow the methodology of Paper I in estimating the symmetry-axis orientation and Thomsen parameters of the effective medium.

Experimental Setup

To simulate a TTI layer, we used XX-paper-based phenolic composed of thin layers of paper bonded with phenolic resin (Figure 1). The experiments were conducted in the Center for Rock Abuse and Physical Acoustics Laboratory at CSM. The measurements were made only in the vertical symmetry plane of the sample, where the velocities and polarizations are described by TI equations (even if the medium as a whole has orthorhombic symmetry). One reflection survey was acquired using flat-faced piezoelectric ultrasonic contact transducers. Another data set was generated by the source transducer and recorded by a scanning laser vibrometer that measures the absolute particle velocity on the surface of the sample.

Seismic reflection experiment

The inversion algorithm of Paper I operates with PP- and PS-waves recorded in split-spread geometry and requires the offset-to-depth ratio to reach at least two. We acquired PP- and PS-wave shot gathers by fixing the source transducer at one end of the model and moving the receiver until the offset reached 30 cm, which corresponds to an offset-to-depth ratio of 2.8 (Figure 1). (Since the sample is laterally homogeneous, shot gathers can be interpreted as CMP gathers.) Then the source was placed at the other end of the model to acquire negative offsets and form a split-spread gather. The same procedure was used to record reflection data with the laser vibrometer.

Vertical component (PP-waves)

The data in Figure 2 were obtained by applying F-K dip filtering to the raw records with the goal of suppressing the ground roll. Evidently, there is close similarity

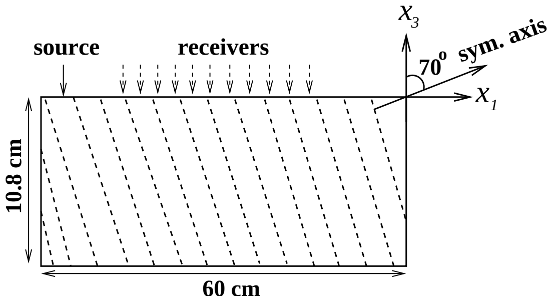

Fig. 1: Physical model representing a horizontal TTI layer. To simulate a reflection survey, the sources and receivers were placed on top of the sample in the symmetry-axis plane.

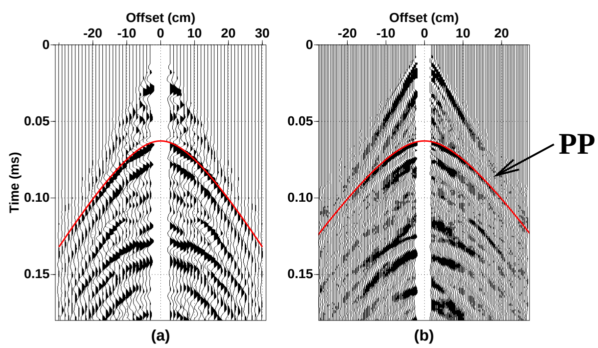

Fig. 2: Vertical component of the wavefield. (a) Data recorded with the P-wave contact transducers; (b) densely sampled data recorded with the laser vibrometer. The solid line is the picked traveltime of the P-wave primary reflection.

between the two data sets (Figures 2a,b) acquired using different experimental setups. The first arrival is the direct P-wave traveling with the horizontal velocity close to 2620 m/s. The P-wave primary reflection from the bottom of the block and the first multiple can be identified at zero-offset times of 0.064 ms and 0.128 ms, respectively. Since the laser dataset (Figure 2b) is more densely sampled and has better coherency, it was used for picking the traveltimes of the PP reflection.

To estimate the P-wave normal moveout (NMO) velocity, we applied conventional hyperbolic velocity analysis after muting out long offsets. The best-fit velocity $V_{\mathrm{nmo},P}$, which flattens the near-offset primary and multiple reflections, is 2350 m/s. At large offsets, the NMO-corrected gather is not flat, which indicates that the medium is anisotropic, and the anisotropy is not elliptical (e.g., Tsvankin, 2001).

Horizontal component (PS-waves)

To clearly identify mode-converted PS(PSV)-waves and pick their traveltimes, we oriented the receiver transducer horizontally in the symmetry-axis plane (Figure 3a). Since the laser vibrometer system could not be used to measure the horizontal wavefield component, we recorded mode-converted SP-waves with the shear-wave source transducer and laser vibrometer and treated the SP traveltimes (according to reciprocity) as those of the corresponding PS-waves (Figure 3b). There was almost no energy on the crossline (transverse) component, which indicates that the data were indeed acquired in a symmetry plane of the medium. Also, we found the shear-wave splitting along the symmetry axis to be negligible, suggesting that the model is either TI or a special case of orthorhombic media (Tsvankin, 2001).

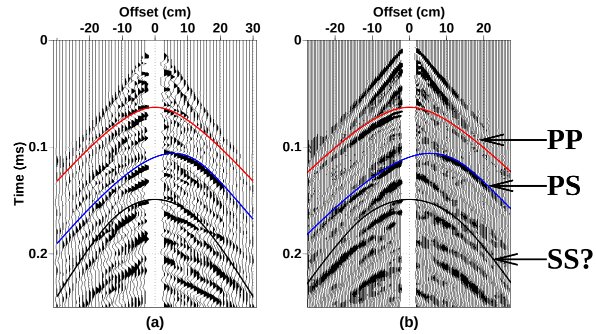

Fig. 3: Horizontal component of the wavefield. Data recorded with: (a) the P-wave source transducer and S-wave receiver transducer; (b) the S-wave source transducer and the laser vibrometer as the receiver. The solid lines are the picked traveltimes of the PP, PS(SP), and SS arrivals. Note the asymmetry of the converted-wave moveout.

The moveout of the mode-converted waves is strongly asymmetric, with a substantial difference between the traveltimes for positive and negative offsets. Since the model is laterally homogeneous, this moveout asymmetry is caused entirely by the oblique orientation of the symmetry axis. The minimum PS-wave traveltime is recorded at an offset of x=6 cm where the wavelet reverses its polarity. To facilitate visual correlation of PS traveltimes, we removed this polarity reversal from the sections in Figure 3.

Data processing

First, we used the PP+PS=SS method (Grechka and Tsvankin, 2002; Grechka and Dewangan, 2003) to compute the traveltimes of the pure SS (SVSV) reflections from the PP and PS data. The traveltimes of both the PP-wave (on the vertical component) and the converted wave (on the horizontal component) were manually picked from the laser vibrometer dataset and smoothed with a sixth-order polynomial using the least-squares method. Then, hyperbolic velocity analysis was applied to the constructed SS arrivals to estimate their stacking velocity ($V_{\mathrm{nmo},S}$ = 1780 m/s) and zero-offset traveltime (t_{S0} = 0.149 ms).

Next, we followed the methodology of Paper I in computing the time (Δt_{PS}) and offset (Δx_{PS}) asymmetry attributes of the PS-wave expressed as a function of the SS-wave offset x_{SS}. The factor Δt_{PS} is determined from the modified PP+PS=SS method as the differences between the traveltimes of the "reciprocal" PS-waves that have the same reflection (conversion) point but opposite

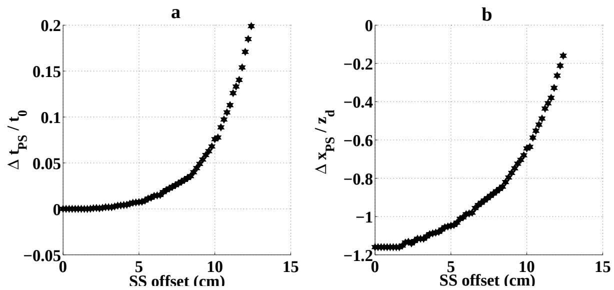

Fig. 4: Moveout-asymmetry attributes of the PS-wave computed from the PP+PS=SS method. (a) The time asymmetry Δt_{PS} normalized by the zero-offset PS-wave time; (b) the corresponding offset asymmetry Δx_{PS} normalized by the layer thickness.

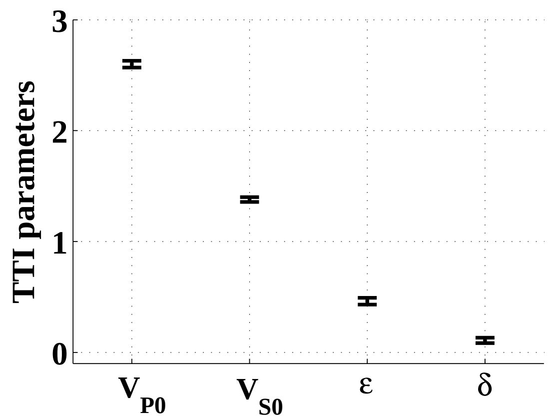

Fig. 5: Thomsen parameters of the sample estimated from 2D PP and PS data in the symmetry-axis plane (the velocities are in km/s). The mean values are $V_{P0} = 2.6$ km/s, $V_{S0} = 1.38$ km/s, $\epsilon = 0.46$, and $\delta = 0.11$. The estimated tilt of the symmetry axis and layer thickness (not shown) are $\nu = 70°$ and $z = 10.9$ cm. The error bars correspond to the following standard deviations in each parameter: 2% for V_{P0}, V_{S0}, and z, 0.03 for ϵ and δ, and 1° for ν.

signs of the horizontal slowness component. Similarly, Δx_{PS} is defined as the sum of the offsets (taking the sign of x_{PS} into account) computed for the reciprocal PS arrivals (Paper I).

The time asymmetry factor Δt_{PS} (Figure 4a) rapidly increases with offset and reaches about 20% of the zero-offset time. In contrast, the depth-normalized offset asymmetry Δx_{PS} reaches its maximum (by absolute value) at small SS-wave offsets (Figure 4b), as predicted by the analytic results of Paper I.

Parameter estimation

The vector $\boldsymbol{d}$ of input data for the inversion procedure includes the NMO velocities and zero-offset times of the PP- and SS-waves and the asymmetry attributes of the PS-wave:

$$\boldsymbol{d} \equiv \Big\{ V_{\mathrm{nmo},P}\,,\, t_{P0}\,,\, V_{\mathrm{nmo},S}\,,\, t_{S0}\,,\, \Delta t_{PS}(x_{SS})\,,\, \Delta x_{PS}(x_{SS}) \Big\}. \tag{1}$$

The model vector $\boldsymbol{m}$ contains the five relevant TTI parameters and the layer thickness z:

$$\boldsymbol{m} \equiv \Big\{ V_{P0}\,,\, V_{S0}\,,\, \epsilon\,,\, \delta\,,\, \nu,\, z \Big\}, \tag{2}$$

where V_{P0} and V_{S0} are the velocities of P- and S-waves (respectively) in the symmetry direction, ϵ and δ are Thomsen anisotropy parameters, and ν (tilt) is the angle between the symmetry axis and the vertical.

To estimate the elements of $\boldsymbol{m}$, we applied the nonlinear inversion algorithm discussed in Paper I. Although both the tilt ν and thickness z were known, they were obtained from the data to simulate a field experiment. To assess the stability of the inversion, the algorithm was applied to 200 realizations of the input PP and PS traveltimes contaminated by random Gaussian noise with zero mean and the standard deviation equal to 1/8 of the dominant period of the signals (Figure 5). All model parameters are well-constrained by the data, with the standard deviations in ϵ and δ limited to 0.03, and the standard deviation in ν close to 1°.

Note that the sample is strongly anisotropic, with the value of ϵ approaching 0.5. The PP- and PS-wave traveltimes computed for the estimated model are practically indistinguishable from the picked traveltimes at all offsets (Figures 2 and 3). Another indication of the high accuracy of the inversion procedure is that the errors in the known values of ν and z are almost negligible.

Transmission experiment

To verify the inversion results using an independent data set, we conducted a transmission experiment by attaching the source transducer to the bottom of the model and recording the wavefield with the laser vibrometer for the full range of angles ($0° - 90°$) with the symmetry axis. For the direct P-wave, the first breaks practically coincide with the traveltimes computed for the inverted model.

The wavefield excited by the S-wave transducer is more complicated and exhibits a cusp at oblique angles with the symmetry axis (Figure 6). For comparison, we employed the spectral-element method (Komatitsch et al., 2002) to compute the wavefield from a horizontal force using the inverted TTI parameters. Although the spectral-element code is 2D, the agreement between the modeled and measured wavefields in Figure 6 is excellent.

The spatial extent of the cusp in Figure 6 is significantly larger than that predicted by the group-velocity surface (i.e., by ray tracing). This is consistent with the observation by Martynov and Mikhailenko (1984) that ray theory underestimates the size of the SV-wave cusp in TI

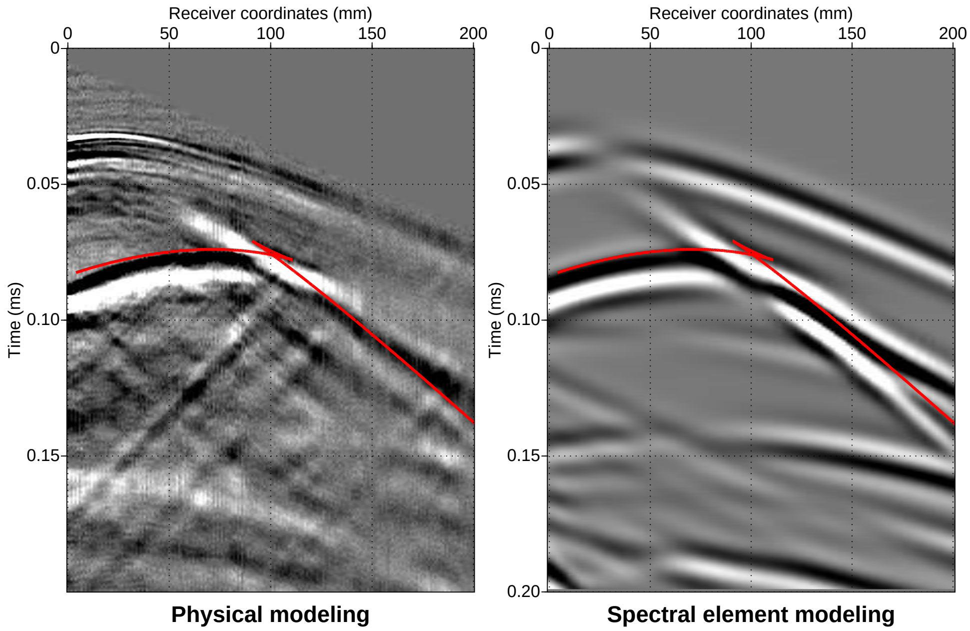

Fig. 6: Cusp (triplication) in the transmitted wavefield excited by a shear-wave source. The wavefield recorded by the laser vibrometer (left) is simulated with the spectral-element method (right). The receiver moves from the direction approximately perpendicular to the symmetry axis (zero coordinate) to that parallel to the symmetry axis. The solid line is the direct shear-wave traveltime computed from the SV-wave group-velocity surface for the inverted model in Figure 5.

media. The deviation of the ray-theoretical S-wave traveltimes (solid line) from the first breaks at offsets larger than 10 cm is explained by the interference of the direct S-wave with the refracted P-wave.

Conclusions

We presented a physical-modeling study of the joint 2D velocity analysis of PP and PS reflections recorded over a TI layer with a tilted symmetry axis. The results confirm the conclusion of Dewangan and Tsvankin (2004) that the combination of the PS-wave time and offset asymmetry attributes with the NMO velocities and zero-offset times of the pure modes makes it possible to estimate all relevant medium parameters. The sample proved to be strongly anisotropic, with the magnitude of P-wave velocity variations approaching 50% ($\epsilon = 0.46$, $\delta = 0.11$).

The PP- and PS-wave traveltimes computed for the estimated model almost coincide with the picked traveltimes at all offsets. Also, the inversion algorithm gave accurate estimates of the known values of the tilt of the symmetry axis and the layer thickness. An independent verification of the inversion results was provided by transmission experiments, which allowed us to record a shear-wave cusp at oblique angles with the symmetry axis. Although the observed cusp is noticeably wider than that on the group-velocity surface calculated for the estimated model, this discrepancy is caused by the inadequacy of ray theory. Full-waveform modeling using the spectral-element method accurately reproduces the cusp and all other major features of the transmitted wavefield.

References

Angerer, E., Horne, S. A., Gaiser, J. E., Walters, R., Bagala, S., and Vetri, L., 2002, Characterization of dipping fractures using PS mode-converted data: 72nd Ann. Internat. Mtg., Soc. Expl. Geophys., Expanded Abstracts, 1010–1013.

Dewangan, P., and Tsvankin, I., 2004, Application of PS-wave moveout asymmetry in parameter estimation for tilted TI media: 74th Ann. Internat. Mtg., Soc. Expl. Geophys., Expanded Abstracts, 861–864.

Grechka, V., and Dewangan, P., 2003, Generation and processing of pseudo shear-wave data: Theory and case study: Geophysics, **68**, 1807–1816.

Grechka, V., and Tsvankin, I., 2002, PP+PS=SS: Geophysics, **67**, 1961–1971.

Komatitsch, D., Ritsema, J., and Tromp, J., 2002, The spectral-element method, Beowulf computing, and global seismology: Science, **298**, 1737–1742.

Martynov, V. N., and Mikhailenko, B.G., 1984, Numerical modelling of elastic waves in anisotropic inhomogeneous media for the halfspace and the sphere: Geophysical Journal of the Royal Astronomical Society, **76**, 53–63.

Tsvankin, I., 2001, Seismic signatures and analysis of reflection data in anisotropic media: Elsevier Science Publ. Co., Inc.